IOP Conf. Series: Materials Science and Engineering **120** (2016) 012010 doi:10.1088/1757-899X/120/1/012010

Hyperband Bi-Conical Antenna Design Using 3D Printing Technique

J.A. Andriambeloson, P.G. Wiid

Electrical & Electronic Engineering Department,University of Stellenbosch, Western Cape, South Africa

E-mail: andyjoely@gmail.com, wiidg@sun.ac.za

Abstract. We combined a 3D printing technique with conductive paint for an antenna manufacturing methodology. The performance of the approach is evaluated through a 3D-printed and coated bi-cone antenna. The antenna far-field pattern and efficiency are measured using near-field spherical scan and reverberation chamber techniques. Good agreement is seen between measurements and simulations and an impedance bandwidth of at least 34:1 is achieved. An extruded bi-conical antenna geometry is also studied for bandwidth extension to lower frequency and an impedance bandwidth of 58:1 is realised.

1. Introduction

Over the past few years, the process of making objects with complex shapes has become easier due to the development and accessibility of open-source 3D-printing machines to the general public. The new tool not only allows an accurate replication of numerical models that are drawn on a computer, but it also permits a light-weight and a low-cost design using plastic materials such as a polylactic-acid (PLA). Here, it is combined with the HSF55 carbon-based conductive paint for low-cost antenna design methodology evaluation. A bi-conical 3D-printed omni-directional antenna is built and is examined to understand the performance of the approach. The study focuses on the antenna under-test (AUT) matching, far-field and efficiency responses. Anechoic and reverberation chambers, as well as computational models are used for validation of the measured antenna parameters.

2. Antenna Under-Test Description

Figure 1.a shows a photograph of our open-source 3D printer printing the truncated cone that was utilised to manufacture the bi-cone antenna in Figure 1.b. The plastic cone is printed with an infill density of 15% using a PLA plastic. A conical machined-piece of aluminium is inserted on top of each truncated-cone (Figure 1.c) and the assembled product is coated with a carbon-based conductive paint: HSF55. The bi-cone is characterised by an angle of 41 degrees for optimal impedance matching over a wide frequency band [1]. It is fed from the bottom of the lower cone through a coaxial cable of 20 cm long as described in Figure 1.c.

3. Antenna Parameters Measurement and Validation

Three antenna parameters are investigated: the bi-cone reflection coefficient (S_{11}), the electric far-field directivity (EFD) pattern and the antenna efficiency. A spherical near-field scan is used

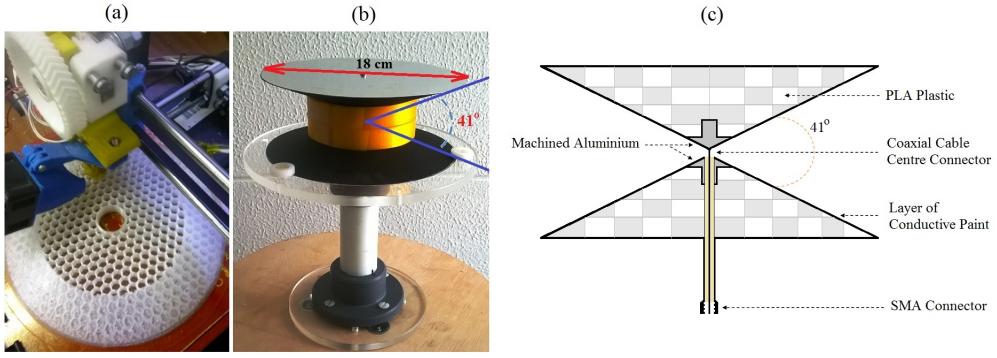

Figure 1. Overview of the 3D-printed bi-cone antenna manufacturing: (a) shows the 3D-printer, (b) displays the finished bi-cone antenna and in (c) is described the antenna feed.

for the radiation pattern investigation while a reverberation chamber technique is employed for the efficiency characterisation. The bi-cone is placed inside our anechoic chamber within the AUT radiative near-field region for the EFD measurement. The AUT normalised EFD pattern is extracted from the spherical near-field data using our anechoic chamber software: NSI2000. As far as the efficiency measurement is concerned, the bi-cone radiation efficiency is derived from the efficiency of a known dipole of 10 cm long that we characterised with FEKO in previous work [2]. Two setup scenarios (S1 and S2) are performed for the investigation and for both, the same radiating antenna is successively placed at the eight corners of the chamber working volume. The power radiated within the chamber is recorded with a vector network analyser (VNA) through the reference-dipole antenna (located at a fixed place) for S1 and through the bi-cone for S2. 72 stirrer steps per revolution are used and the bi-cone efficiency is calculated using the average of the 72×8 S_{21} matrix collection as expressed in (1). It is also important to notice that here each S_{21} is corrected from port mismatches.

$$\eta_{Cone} = \eta_{Dipole} \frac{< |S_{21\,(S1)}|^2 >}{< |S_{21\,(S2)}|^2 >} \tag{1}$$

For the bi-cone simulation, the paint coating was modelled using a uniform layer of perfect electric conductor (PEC), aluminium and the CST predefined graphite material. The PEC provides the idealised antenna response while the aluminium and the graphite allows us to inspect the variation of the antenna radiation when the coating layer conductivity changes.

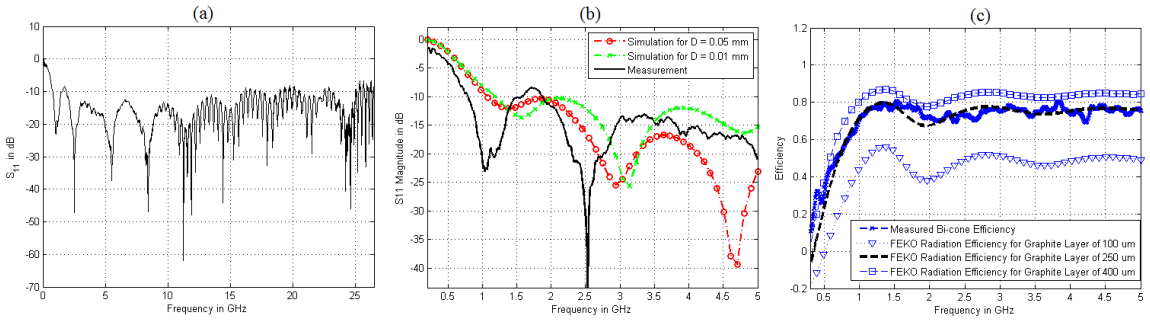

Figure 2. Reflection coefficient of the bi-cone antenna: (a) shows the measured S_{11} using a 26.5 GHz Agilent PNA-X VNA and in (b) it is compared with simulated curves up to 5 GHz. (c) displays the measured and the simulated antenna radiation efficiencies.

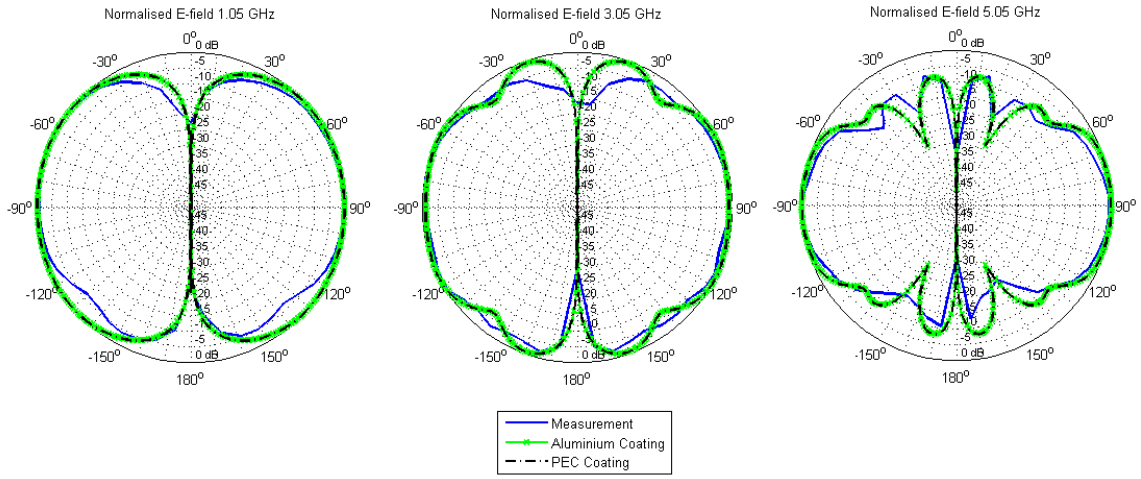

Figure 3. Comparison between measured and simulated bi-cone normalised EFD for 1.05 GHz, 3.05 GHz and 5.05 GHz.

4. Results and Discussion

Figure 2.a shows the antenna S_{11} as measured with a 26.5 GHz Agilent PNA-X VNA. Using a matching threshold of -10 dB, the bi-cone achieved an impedance bandwidth of at least 34:1. The measured S_{11} is compared with simulation results up to 5 GHz on Figure 2.b. Here, a good agreement is seen between the curves in terms of shape and level, but different resonances are observed. This behaviour is expected since the antenna S_{11} is influenced by the gap spacing (D) between the upper and the lower cones as found in [1]. The model coating thickness has been adjusted to fit the measured efficiency result and a graphite layer of 250 m thick was found to be the best match for the physical antenna coating (see Figure 2.c).

Figure 3 compares the measured and the simulated normalised EFD of the bi-cone antenna for 1.05 GHz, 3.05 GHz and 5.05 GHz. The bi-cone main-lobes agree with computations between -60 and 60 degrees, but clear deviations are observed within the side-lobe regions located around 0 and 180 degree. The overall simulated far-fields are symmetric relative to the horizontal line of the polar axis, but no symmetry is observed for the measured curves coloured in blue. This observation is clearly shown by the curves for 1.05 GHz and this is due to an unbalanced feed problem where common-mode currents flow over the feed-cable external conductor and radiate unwanted energy in the antenna surrounding. The unbalanced-feed issue can be solved using a balun or a differential amplifier, but these solutions are not appropriate for the bi-cone due to its hyperband response. A different approach is necessary to reduce the feed-cable effect and this will be investigated in further work.

5. Antenna Response Improvement for Low-Frequency Signals

The low-frequency limit of the bi-cone antenna can be extended using a larger cone-radius. However, our 3D-printer cannot print a conical structure having a radius more than 9 cm. Another technique had to be investigated and here, we used an approach which is similar to the one presented in [3]. We extruded the base of each cone by a height H to allow the bi-cone to act as a dipole antenna at low-frequency (see Figure 4.a). Four FEKO models were used for the study where the height of the cylindrical expansion (H) was varied from 4 cm, twice the cone height L, 8 cm and 10 cm. The simulated S_{11} are shown in Figure 4.b. We can see here that the extrusion of 8 cm provides the lowest cut-off frequency and where the antenna S_{11} remains less than -10 dB from around 450 MHz. Two new bi-cones have been realised using a cone-radius

of 8.57 cm to physically check the effectiveness of the extrusion technique. The first antenna is similar to the previous bi-cone while the second was manufactured using the extrusion value of 8 cm found earlier. The S_{11} of both antennas were measured and are compared with simulations in Figure 4.c. The two measured S_{11} agree with simulation results and a low-frequency limit shift is observed from 1.18 GHz to around 450 MHz due to the cylindrical expansion. The extruded bi-cone works up to 26.5 GHz and this increases the antenna impedance bandwidth to at least 58:1.

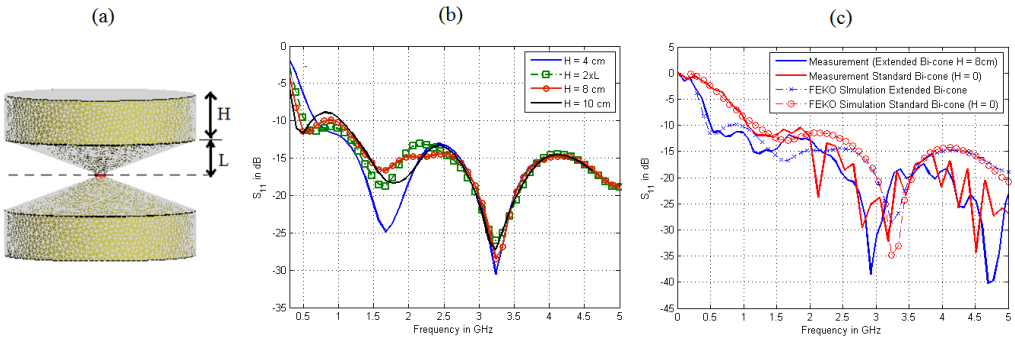

Figure 4. Description of the bi-cone extrusion technique for low-frequency limit improvement. (a) and (b) show the computational model and the simulated S_{11} for four extrusion values. (c) compares our measurement results with simulation using a cylindrical expansion of 8 cm.

6. Conclusion

With low-cost in mind, a 3D-printed bi-cone antenna was manufactured to investigate the performance of a 3D-printing technique and conductive paint for an antenna manufacturing methodology. The antenna S_{11}, electric far-field pattern and efficiencies were measured, using anechoic and reverberation chambers, and obtained results were validated using simulations. A uniform graphite layer was used to model the antenna coating layer and this provided a good agreement with measurement results. The current antenna design achieved a -10 dB impedance bandwidth ratio of 34:1 (770 MHz to 26.5 GHz). An efficiency of more than 70% was measured with the reverberation chamber technique up to 5 GHz. The low frequency cut-off of the bi-cone was also improved using a cylindrical extrusion technique and our current prototype achieved an impedance bandwidth of 58:1. The study shows the effectiveness of the 3D printing technique and the HSF55 conductive paint for antenna design, but further work is necessary to solve the antenna unbalanced feed issue. In this regard, a combination of L-plates and absorbers will be investigated to attenuate the flow of common-current across the feed-cable external conductor.

Acknowledgement

We acknowledge the following people for their help in the work: Dr H. Pienaar, Mr W. Croukamp, Ms A. Bester, MeerKAT team, Altair-FEKO and CST, SKA-South Africa and SARCHI for funding.

References

[1] Wiid P. G. *The Answer is in Fact 41, or How to Get 35:1 Bandwidth from a Cone Antenna, Int. Conf. on Antenna and Propagation in Wireless Communications (APWC)*, pp 1060-1063,Turin, Italy, 7-11 Sept 2015.
[2] Andriambeloson J. A. *Reverberation Chamber Time and Frequency Metrology for MeerKAT Systems Shielding Evaluation*, Chap 3, pp.26-42, Dec 2014, http://hdl.handle.net/10019.1/96037.
[3] Keller S. D. *Wire-Frame Monocone Antenna for Direction-Finding Applications on Unmanned Aerial Vehicle Platform, Antennas and Propagation Magazine*, IEEE, vol.53, no.1, pp.56,65, Feb. 2011.